

HawkVision: Low-Latency Modeless Edge AI Serving

ChonLam Lao
Harvard University

Jiaqi Gao
Harvard University

Ganesh Ananthanarayanan
Microsoft

Aditya Akella
UT Austin

Minlan Yu
Harvard University

Abstract

The trend of modeless ML inference is increasingly growing in popularity as it hides the complexity of model inference from users and caters to diverse user and application accuracy requirements. Previous work mostly focuses on modeless inference in data centers. To provide low-latency inference, in this paper, we promote modeless inference at the edge. The edge environment introduces additional challenges related to low power consumption, limited device memory, and volatile network environments.

To address these challenges, we propose DragonEye, which provides low-latency modeless serving of vision DNNs. DragonEye leverages a two-layer edge-DC architecture that employs confidence scaling to reduce the number of model options while meeting diverse accuracy requirements. It also supports lossy inference under volatile network environments. Our experimental results show that HawkVision outperforms current serving systems by up to 1.6 \times in P99 latency for providing modeless service. Our FPGA prototype demonstrates similar performance at certain accuracy levels with up to a 3.34 \times reduction in power consumption.

1 Introduction

The increasing demand for machine learning inference in applications like vision [54, 62], chatbots [22, 69, 70], and other interactive applications [30, 55] has garnered significant attention. Amazon reports that over 90% of costs arise from inference [1, 2]. To provide low-latency services, edge prediction serving systems are widely deployed [6, 7, 18, 30, 57] to reduce the distance between end-users and the data center and mitigate the increasingly complex computational costs (e.g., inference preprocessing cost).

As the demand for inference increases and user requirements become more diverse, *modeless* prediction serving has become prevalent [28, 38, 63]: Developers pre-register models with various accuracy requirements to the serving system beforehand. When users send inference requests, the serving system selects the appropriate model to satisfy users' requirements.

Accuracy requirements vary significantly among applications, such as bank app face verification (which requires high accuracy) and social media face recognition (which requires

lower accuracy), even though both involve the same face recognition task [61, 63]. Furthermore, different pricing systems and user tiers (e.g., free users vs. enterprise users) make serving different accuracy requirements increasingly popular. The trend of allowing modeless serving delivers better granularity for both users and service providers, thereby lowering service costs and aligning with users' desired requirements. The serving system should satisfy different users' requirements at the lowest possible cost.

Yet, building such *modeless* inference systems for edge serving support is not easy. Previous work [28, 63, 79] widely discusses modeless serving in the cloud with lower latency and lower deployment costs. As latency becomes crucial for prompt and predictable performance and meeting SLOs for users, edge serving system is receiving more attention [6, 7, 42, 57, 66]. However, few studies discuss edge deployment for modeless serving. The challenges are as follows:

Challenge ①: Serving a wide range of accuracy requirements at the edge is expensive. To meet diverse accuracy requirements from users, we need to provide a sufficient number of model options to the serving system. Otherwise, if we have to use an overkill model for an application with low accuracy need, we incur unnecessary inference computational costs. MLPerf [61] shows that choosing a model with slightly higher accuracy (e.g., a few percent) can lead to 5-10 \times computational costs. Therefore, it is important to host a wide range of models for various accuracy needs and dynamic workloads.

However, hosting many models concurrently is impossible given the limited memory at edge GPU and CPU [18, 57]. Therefore, we have to load pre-registered target serving model options in the runtime [34, 57, 77, 79], but frequent runtime model loading (cold-start inference) between GPU and CPU can introduce unpredictable latency and result in low GPU utilization. Recent research indicates that the load time versus the inference time can be up to 3:1 [34].

Challenge ②: The volatile network environment of edge serving. The edge network environment is often unreliable due to poor network quality caused by multi-tenancy and bursty behavior in the wild, leading to unpredictable and high tail latency due to queuing or retransmission at the edge [52, 81]. Moreover, real-world inference-serving workloads exhibit burstiness with extremely high short-term

variance [77–79], putting more pressure on the edge network during serving. These network challenges significantly contribute to high end-to-end inference times (as discussed in Section §2.2).

Challenge ③: Serving ever-growing processing costs at the edge. Unlike data centers, edge inference systems have significantly fewer resources and power supplies [42, 44, 57]. However, even a low-end GPU (e.g., Nvidia T4) can consume up to 75W, which creates pressure for widespread deployment in edge environments. Inference processing tasks are becoming increasingly complex, encompassing tasks such as JPEG decoding and other image preprocessing functions, which contribute to nearly 32-59% of the end-to-end inference latency (as discussed in Section §2.3). Achieving both *low latency* and *low power consumption* simultaneously can be challenging.

To address these challenges, we propose HawkVision, which provides low-latency modelless serving of vision DNN. There are three key designs in HawkVision:

First, we propose *confidence scaling*. Instead of switching models at runtime for different target models, which can incur high swapping costs or lead to serving with an overkill model ①, we employ only a dual-model approach to navigate the accuracy space. When we receive a request, it is sent to two models concurrently: a lightweight model serves as the frontend, promptly addressing easy requests and obtaining the output "confidence score". If the confidence level exceeds a certain *confidence threshold* (deemed trustworthy), the response is directly sent back to users, and the backend powerful model is notified to stop inference; otherwise, we wait for the fallback on the backend powerful model to produce the inference results. The *confidence threshold* provides a tunable knob for serving systems to accommodate a wide range of accuracy requirements with only two models at a minimal cost. The edge is suitable for deploying a lightweight and static model as the frontend; while the cloud can host the backend powerful model.

Second, to reduce network delay in an unreliable network environment ②, we propose a hardware-friendly *unreliable* transport layer at the edge that allows *lossy JPEG recovery* in a streaming manner when packet loss occurs. This enables inferences with partial information (e.g., inference on images with missing pixels) to reduce latency and avoid retransmission costs. Combined with *confidence scaling* and fallback mechanisms, we do not need to sacrifice accuracy.

Third, we build our system in an edge-DC setting, with the frontend deployed at the edge and the backend placed in the data center. Our main system are on GPUs for both the frontend and backend. We also build an FPGA frontend prototype which not only hosts the lightweight model, but also supports the entire inference pipeline from packet processing,

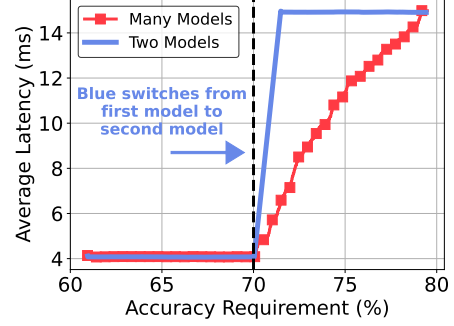


Figure 1. Serving different requirements with two models

network stack, and data preprocessing. Our FPGA prototype further verified the feasibility of implementing both *confidence scaling* and *lossy JPEG recovery* in a low-power hardware, showing low latency and high power efficiency compared to GPU solutions.

Our evaluation shows that HawkVision achieves up to $1.37\times$ improvement in P90 latency and $1.6\times$ improvement in P99 latency compared to Clockwork serving modelless in a multi-tenancy environment with different hardware profiles. Our FPGA also demonstrates up to $1.5\times$ and $3.34\times$ reductions in power consumption while serving the same 75% accuracy requirement.

2 Motivation and Challenges

Modelless serving offers applications with various user-specified accuracy requirements, posing challenges to the underlying serving system (§2.1). The poor network conditions (§2.2) and the limited resources and power constraints (§2.3) at the edge make serving even more difficult.

2.1 Serving Applications with Diverse Accuracy Requirements

Different models have different accuracy and latency variants [61, 63]. The right selection and use of these variants are crucial for modelless serving. However, serving a massive amount of model options with varying requirements introduces high swapping costs during runtime. Even in image classification tasks alone, there are at least 44 vision models available, each offering varying trade-offs between computation and accuracy within an accuracy range of 55% to 83%[61]. Since GPU memory is expensive, models cannot be stored in GPUs all the time. Instead, these models are loaded into main memory and scheduled to meet the Service Level Objective (SLO) during runtime. However, frequent loading and unloading of models during runtime can result in unpredictable latency. Clockwork[34] shows that the model transfer time between GPU and CPU can be up to $3X$ the model inference time. This runtime cost accumulates in the client end-to-end latency if the model is not loaded

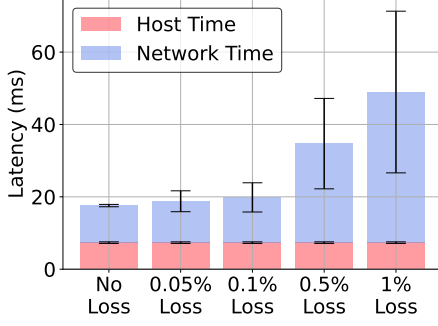


Figure 2. Impact of Packet loss

(cold inference). Moreover, real-world workloads are highly dynamic [49, 78], and it is difficult to predict the workloads accurately. Incorrect estimation of the demands for specific models can lead to significant runtime GPU resource scaling and allocation issues.

In contrast, failing to provide a sufficient number of models to express the spectrum causes a lack of granularity in model selection, which results in using overkill models to address simpler demands, leading to unnecessary inference costs.

In the following experiments (Figure 1), we demonstrate the drawback of using an overkill model to serve requests with different accuracy levels. We modify Clockwork [34], a state-of-the-art serving system, to support modelless. We pre-register two models provided in the Clockwork repository into the serving system to accommodate different accuracy requirements, namely *winograd_resnet18_v2* (with 70.65% accuracy) and *resnet101* (with 82.17% accuracy). We use this setup to compare with another run where a massive amount of models with different accuracy levels are loaded into the system to serve varying accuracy requirements. This experiment does not incur any swapping latency.

We initialize 4000 requests with varying accuracy requirements, ranging from 60% to 80%, in ascending order, and send them to the serving system. The serving system selects the model that can provide sufficient accuracy for each request. In the original system, with around a 70% accuracy requirement, the average latency significantly increases due to the serving system switching to an overkill model. The result shows that the use of many models provides better model allocation, resulting in improved average latency than using two models.

2.2 High Network Overheads on Edge

High tail latency and packet loss are common issues encountered in edge networks due to the increasing trend of multi-tenancy and bursty behavior during peak usage times [19, 52, 81].

Tail latency is the primary cause of performance reduction. AUGUR [81] demonstrates that in edge settings, long latency

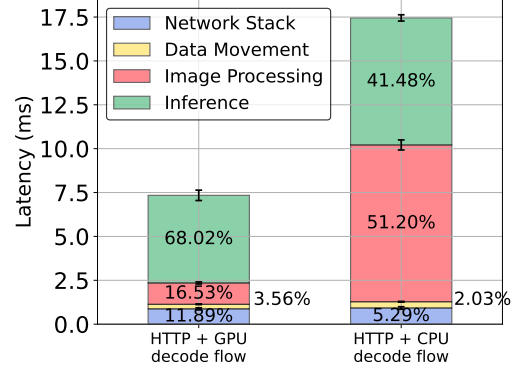


Figure 3. Breakdown of inference latency with 0ms network delay

is observed, with the median round-trip time (RTT) staying below 30ms, while the 99.9th percentile latency exceeds 200ms. These long tail latencies stem from RTT inflation induced by fluctuations in edge wireless paths. Another network problem is edge packet loss [52]. This occurs when the number of users is high or the quality of the wireless environment is poor [19], and it typically dominates the end-to-end delay of inference.

Packet loss is another performance killer. To demonstrate how packet loss affects inference performance in edge, we conducted an inference task on the ImageNet dataset [29] using the state-of-the-art ConvNet model [50] on the Nvidia A100 GPU. Figure 2 illustrates the impact of network loss on inference time with a 10ms network delay and loss rates ranging from 0.05% to 1%. With 1% packet loss, the inference time increases by 4× compared to no packet loss. This delay occurs because it takes several round-trips to recover lost packets before the full image can be decoded and inference can begin. Notably, the network time significantly exceeds the computation time.

2.3 The Need for High Performance in Complex Tasks with Limited Resources

Apart from inference, preprocessing tasks contribute a significant portion of the end-to-end delay. Addressing both model inference and preprocessing tasks with high performance and accuracy is challenging, especially with the limited resources at the edge.

In Figure 3, we measure the breakdown of the average inference latency at the host in an image classification task with the same setting as in Section 2.2, with network delay set to 0. In the HTTP + CPU decoding workflow, the inference time constitutes only about 41.48%, with the remaining time consisting of (1) **HTTP/gRPC and TCP stack processing (5.29%)**, which would further increase if we experience long network delays and/or packet loss, as demonstrated in 2.2.

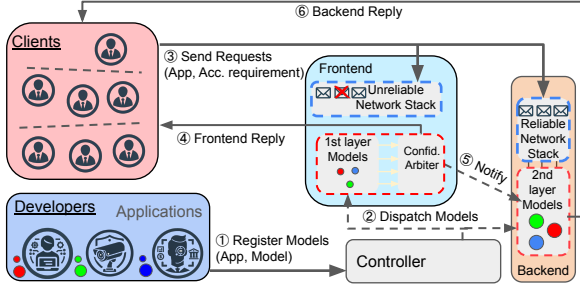


Figure 4. HawkVision Overview

(2) **Data movement (2.03%)**, although it represents a small portion in the classification task, it is worth noting that it incurs a non-negligible cost when the inference task is communication-intensive or simple, as shown in [67], due to multiple data transfers among NIC, CPU, and GPU. (3) **JPEG image decoding and preprocessing (e.g., cropping, centralizing) (51.20%)**, as clients typically send data in a compressed format to reduce communication volume. If we optimize the JPEG decoding task to use GPU hybrid [9], the additional network stack and data processing time still account for approximately 32% of the total inference time, in addition to incurring an extra 20% in GPU utilization costs (not reflected in the figure). This breakdown applies to other image processing tasks and reliable network protocols used in inference frameworks (e.g., gRPC).

When comparing the GPU and CPU decode workflows, it becomes evident that the majority of time is spent on JPEG decoding and inference, with GPU-based JPEG decoding offering significant advantages. However, in edge settings, GPU options are limited due to power supply constraints, while CPUs are often too weak to handle such computations.

3 Overview

To address the challenges of model deployment (§2.1), network (§2.2), and performance efficiency (§2.3), we propose HawkVision. HawkVision’s goal is to provide a *low end-to-end inference latency* serving system for applications with diverse accuracy requirements and user workloads. It also aims to *minimize deployment resources* to best fit edge scenarios.

Our key insights of HawkVision designs are as follow:

Hierarchical inference with confidence scaling: Applications have different accuracy requirements according to their user needs or pricing schemes. To serve a wide range of accuracy requirements at low cost, we employ a hierarchical architecture that utilizes two models for each application: the frontend includes small models, providing ultra-low latency but moderate-level accuracy to serve requests initially, and the backend uses large models with the best accuracy.

Both models process the request concurrently, if the frontend has high confidence in its response, it sends a cancel to the backend model to reduce cost. Otherwise, the frontend drops its response and waits for the backend to propose a high accuracy result. This approach allows us to reduce both the latency and cost needed to process requests with diverse application requirements without losing accuracy.

Unreliable transport that tolerates packet loss and high tail latency: To reduce the network overhead associated with handling packet loss, reordering, or tailed packets, we propose running unreliable transport within the frontend. Our lossy inference design supports a hardware-friendly, streaming-based corrupted JPEG image recovery scheme to enable making inferences with partial information, tolerating packet loss, and disregarding tailed packets in a low-quality or long-distance Internet network connection.

The key benefit of such a frontend-backend design approach is that it has minimal impact on the original inference network protocols and inference models at backend hosts while allowing for innovation on the frontend design. This ensures compatibility with different inference frameworks. If the frontend fails, the original inference backend can still continue to work.

We also demonstrate the feasibility of implementing the two core ideas above in a cost-effective full-stack FPGA prototype. This is because data processing and inference overhead contribute significantly to the end-to-end time, and there is room for improvement in power consumption and performance with GPUs. By leveraging the specialization of FPGA architecture—such as handling streaming-friendly tasks like JPEG decoding or avoiding multiple PCIe transmissions among CPU, GPU, and NIC—latency can be reduced. Additionally, the use of FPGA can be more cost-effective and consume less power compared to GPUs, which is beneficial for edge deployment where power and memory constraints are typically tight.

Figure 4 shows HawkVision’s workflow. There are two components in HawkVision: the frontend and the backend. In the preparation phase, developers first need to register applications with two models in our controller ①: a lightweight model in the frontend and a powerful model in the backend. Once the dual models have been registered, the controller calculates the corresponding accuracy requirement with the required confidence thresholds, determining how confident the answers need to be to be directly sent back to the client by the frontend. When a user sends a request with a accuracy requirement, we map it to that confidence threshold for the request to achieve the desired end-to-end accuracy ②.

After the preparation phase, clients send inference requests for their applications with different accuracy requirements to both HawkVision’s frontend and backend ③. The

frontend uses an unreliable network stack and a small model to handle packet loss, recover images, and perform lossy first-layer inference, while the backend uses a reliable network stack and a powerful model as the original setting. When the inference result is too difficult for the frontend (which might be due to a difficult request or the frontend’s small model lacking confidence due to lossy inference), it falls back to the backend for inference.

If the HawkVision frontend is able to handle the request with confidence, it directly sends the result back to the client ④ and notifies the backend to terminate the ongoing inference ⑤. Otherwise, it waits for the backend inference to complete and sends the final result back to the client ⑥.

In the following sections, we discuss the use of confidence scaling (§4) and our unreliable transport design (§5) to achieve low deployment cost and low latency. We then introduce how we implemented these two ideas into our system and the FPGA prototype (§6) to achieve high power efficiency.

4 Confidence Scaling

We use confidence scaling to cover the entire accuracy spectrum for modeless serving. First, we discuss the root causes of the two-end puzzle faced by existing modeless systems, followed by justifying the use of the confidence score and confidence threshold. Finally, we describe how this approach helps us achieve inference at request-level accuracy.

4.1 Problem Observation

Modeless serving is challenging. Typically, the serving system can only serve models that developers pre-registered, and it does not have permission to access the models. If we register many model options to serve different accuracy requirements, it will lead to a high swapping rate because the accuracy requirement varies over time. If we register insufficient model options, we will easily serve requests with overkill models, as discussed in §2.1.

In general, such inference systems face the two-end puzzle between the high model swapping rate and unnecessary inference latency overhead. We observe that this two-end puzzle stems from the use of *per-model granularity* of accuracy in existing serving systems.

HawkVision introduces confidence scaling to resolve the puzzle mentioned above. We use the confidence score output from the lightweight model to estimate the confidence of the request’s answer and determine if it should be sent to the backend model. This approach provides two benefits: (1) We control the proportion of requests sent to the backend, creating a mechanism for achieving the entire spectrum of end-to-end accuracy requirements. (2) The relationship between high confidence and correct answers allows for better labor division between the frontend and backend, enabling

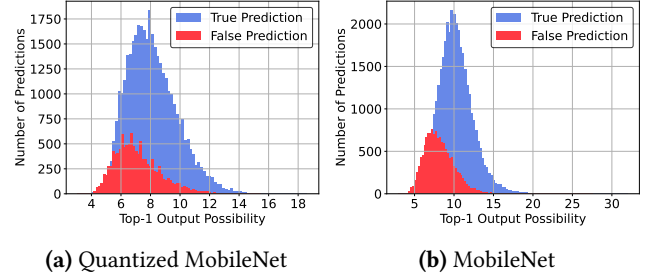


Figure 5. Top-1 possibility distribution of true/false predictions of two models

the frontend to directly handle requests when it is deemed trustworthy.

Previous works [6] employ confidence scaling to handle requests in a cascading manner: a lightweight model handles easy requests, while difficult requests from the frontend are forwarded to a more powerful backend model when the confidence score is insufficient. Although the basic idea is similar, our use of confidence scaling aims to create an accuracy spectrum to minimize the serving system cost in response to the increasing demands for serving different accuracy requirements, rather than focusing solely on inference performance considerations.

4.2 Use of Confidence and Justification

There are different ways to determine the confidence of an answer given by the model. In HawkVision, we use the last softmax layer of the CNN model and select the N-th highest probability as the result’s confidence score when the inference job selects the top-N outputs. This confidence score is model-local, easy to obtain, and simple to calculate. Other methods of calculating the confidence score and different applications, such as language models, are discussed in §9.1.

Previous works [36, 53, 72] have shown that recent models are well-calibrated and the output possibility vector can correctly reflect the confidence of the inference results.

To demonstrate this, we choose the MobileNet and its quantized version as examples and show the top-1 output possibility and the distribution of true and false predictions. The result is shown in Figure 5. In both models, true predictions have an overall higher confidence score than false predictions. Next, we look at quantized MobileNet and show the effect of confidence thresholds. We gradually increase the confidence threshold and accept the result only when the top-1 possibility is above the threshold. Figure 6 shows the percentage of inference requests accepted and the corresponding accuracy. When the confidence threshold increases, fewer requests are handled by the light model but the accuracy goes higher.

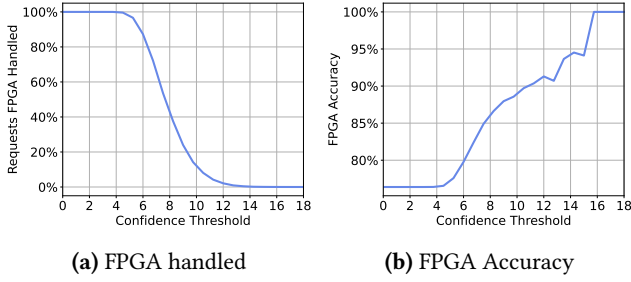


Figure 6. FPGA in different confidence threshold

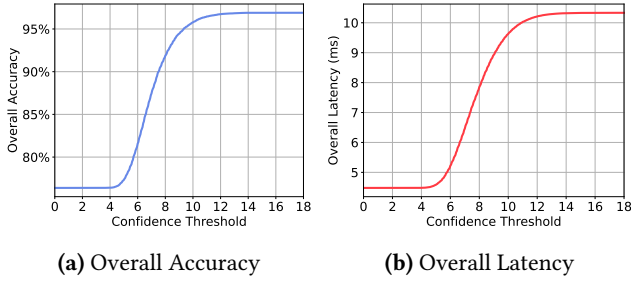


Figure 7. Overall Accuracy v.s. Latency

The confidence threshold offers a knob for the operator to choose the number of inference requests intercepted by the frontend, which balances between inference latency and accuracy: a lower confidence threshold offloads more work to the frontend, which lowers inference latency at the cost of lower accuracy, and vice versa. Figure 7 shows the latency and accuracy trade-off under different confidence thresholds. The operator can set a target latency or accuracy goal accordingly. For example, when the frontend only handles top 50% high score requests, the accuracy increases from 76% to 85%.

5 Lossy inference

In order to handle requests with missing information due to packet loss without retransmission, we develop HawkVision loss-tolerant protocol to help the frontend recover from data loss and make inferences based on partial results while minimizing negative impact.

To reduce the bandwidth consumption between the client and the GPU server, all the images are encoded in compact formats such as JPEG before being transmitted. This makes the image loss-prone: one single packet loss can dramatically reduce the inference accuracy and sometimes even destroy the image and terminates the current inference job on the frontend. The low latency requirement forbids the frontend from waiting for the retransmitted packets. Naively filling the lost gap with zeros or duplicating the previous packet does not help because the encoded format is damaged.

The fundamental reason is that the transport layer has no knowledge about the format of the image. So the lost packet does random damage to the transmitted image and cannot be recovered. We take JPEG, one of the most commonly used encoding formats as an example to demonstrate how HawkVision aligns the packet with the JPEG Minimum Coded Unit (MCU) to constraint the burst radius of packet losses and keep the image recoverable.

The next challenge is how to recover lost information in the frontend. The goal of such recovery is to minimize the accuracy drop of the inference model on FPGA. So instead of filling zeros following the JPEG format, HawkVision chooses to fill the lost information with MCUs already received. The similarity between the packets within the image can help reduce the accuracy drop.

In this section, we first introduce the JPEG format, and the special packet format HawkVision used on the client side to constraint the burst radius of the lost packet, then in the frontend, we explain the JPEG recovery model that restores the image and reduces the inference model’s accuracy drop under loss.

5.1 JPEG encoding format

One JPEG image has two sections: the header and the encoded payload. The header stores the encoded image’s meta-data (such as dimension, customized application data, *etc.*) and a collection of necessary information for the decoder. The header is crucial to image decoding and the image is not recoverable if the header is damaged. Since the header is relatively short compared with the encoded payload (usually less than 1%), HawkVision does not protect or recover the JPEG header if it is lost or partially lost. Our focus is the encoded payload.

The basic unit of encoded payload is Minimum Coded Units (MCU). An MCU contains the compressed pixels of a square block (such as 8x8 pixels) in the original image. Its length varies depending on the content in the block and it is not byte-aligned. Usually, an MCU’s size is tens of bytes, and the encoded payload contains hundreds to thousands of MCUs. Each MCU is encoded based on the delta of the previous MCU. Different MCUs are encoded independently, this means the decoding pipeline is not interrupted if one entire MCU is missing. However, if an MCU is lost partially, since the MCU information is compressed, it is impossible to recover the partially lost content. To make things worse, the decoding pipeline is affected since the decoder cannot recognize the mismatched packet format. This creates a huge ‘burst radius’: one single packet loss in an image can corrupt the entire decoding pipeline.

Ignoring the missed MCUs is not an option, since the decoder continuously consumes the follow-up packets’ content until it believes it has found all MCUs declared in the

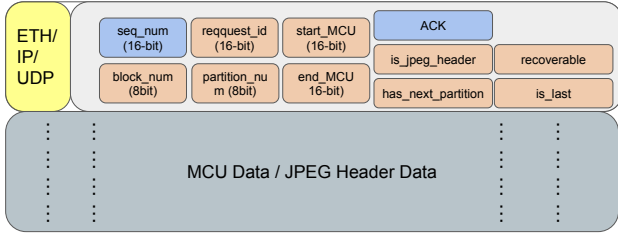


Figure 8. HawkVision packet format, orange fields are for loss recovery protocol and blue fields are for reliability between clients and GPU servers.

header’s metadata. This further expands the burst radius across multiple images.

5.2 JPEG-aware packet packing

To prevent the image decoding pipeline from being interrupted by packet loss, we propose the JPEG-aware packet packing. The transport layer is aware of the sent image’s encoding format and the sent packets are aligned with MCU as much as possible. However, this is not easily achievable since a packet is always byte-aligned but an MCU is not. To solve this problem, we propose a new byte-aligned layer atop the MCUs — *MCU Block*. An MCU block contains multiple MCUs and always ends with a byte-aligned MCU. The MCU block is the basic recovery unit. One MCU block may cross multiple packets, and if one of the packets is lost, the entire block is discarded. We first present how HawkVision constructs packets and the necessary information in the header to guide image decoding, next, we explain how the image is recovered when a packet is lost.

5.2.1 Packets Construction

The guideline for designing the header format and packet construction process is to provide as much information as possible to simplify and accelerate the processing pipeline. This helps avoid additional processing in the frontend, which stalls the pipeline and increases the inference latency.

Before sending the packet, the sender examines the image according to the JPEG format and splits the image into header and multiple MCU blocks. Next, HawkVision constructs the sent packets by packing each MCU block into as few packets as possible, then set the following header fields, as shown in Figure 8:

- *request_id*. The unique ID of each inference request.
- *start_MCU* and *end_MCU*. The start and end MCU IDs in the MCU block. This helps the frontend to recognize if MCUs are missing and how many are missed so that they can be recovered accordingly.



(a) Intact Image

(b) Recovered Image

Figure 9. Original and recovered images

- *block_num*. Indicates which block the packet belongs to, *i.e.* whether the packet belongs to the current MCU block or the next one.
- *partition_num*. Indicates how many packets the MCU block is split into. This tells the FPGA how many packets should be expected since frontend has to drop the entire MCU block if any packet is missing.
- *has_next_partition*. This 1-bit field denotes whether the next packet belongs to the same MCU block.
- *is_peg_header*. If the current packet contains the JPEG header, this 1-bit field is set. Because the JPEG header is not recoverable, if lost, the frontend skips the current image, clears the cache, and lets the backend handle the inference.
- *is_last*. This indicates the last packet of the image and triggers the image recovery pipeline if any packet is lost during transmission.
- *recoverable*. If the image is too small, HawkVision cannot find an MCU block or there is only one such block. This bit is used to notify the frontend to flush the entire image when any packet is lost because such an image is not recoverable.

5.3 JPEG Loss recovery

Upon receiving the first packet of the image, the frontend examines whether the *is_peg_header* field is set, if not, the header is lost during transmission and the image is not recoverable, all subsequent packets with the same *request_id* are ignored. Otherwise, the frontend proceeds the decoding and recovery procedure. The frontend stitches packets together into MCU blocks by examining the *has_next_partition*, *block_num*, and *partition_num* fields. If any packets are lost, the frontend records how many MCUs are lost and discards the entire MCU block.

Recovery pipeline. As introduced in Section §5.1, the frontend has to fill the lost MCUs to prevent the decoder from corrupting the next image. HawkVision chooses the smallest received MCU as the recovery MCU to protect the decoding pipeline from corruption. There are two ways to insert the recovery MCU.

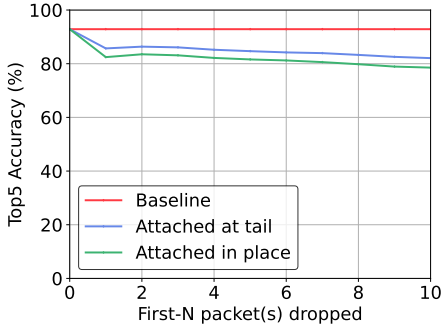


Figure 10. First-N-packets drop

The naive solution is to insert the recovery MCU directly after an MCU block is discarded. However, since the recovery MCU is randomly chosen in the image, filling in wrong information can propagate the error to the rest of the image, lowering the accuracy of the inference model. Instead, HawkVision chose to fill the MCU at the end of the image. This leverages the spatial similarity between nearby MCU blocks and minimizes the impact of the lost information. Figure 9 shows the original image and the recovered one when one packet is lost during transmission. The objects in the image are still recognizable, and the inference model in the frontend also returns the same correct answer.

To further study this, we set up an inference service that runs the ResNet50 model and tested it with the ImageNet dataset. We dropped the first N packets for every image during transmission under different loss rates and recovered it through the two above recovery procedures. The first N packets impact the images most because all the following MCUs’ delta values are changed.

The average image size of the ImageNet is 130k bytes. The result shows even if 10 packets are dropped (around 13k bytes, nearly 10%), the model remains around 80% of top-5 accuracy. Attaching the lost MCU at the tail of the image gives another 4% accuracy boost compared with attaching them in place.

6 Implementation

The HawkVision implementation consists of (i) a client that launches inference requests, (ii) a frontend edge inference box, (iii) a backend DC inference server, and (iv) an additional FPGA frontend prototype. We will open-source the code for all components after review [3].

6.1 GPU-based System

Client. The client launches prediction requests. We develop a communication library handles the image input from the users. The library has two main functions: (1) collecting the necessary metadata from the image to support a loss-tolerant protocol. This part is based on libjpeg-turbo [5] to

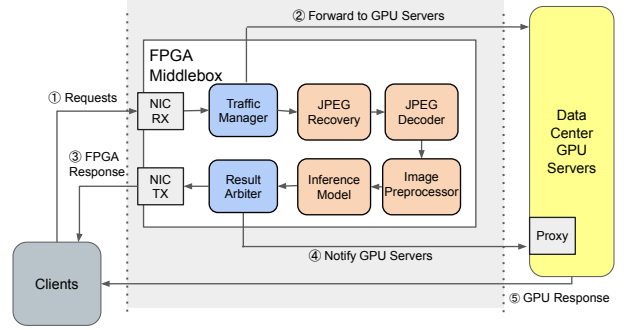


Figure 11. HawkVision-FPGA Implementation Overview

analyze the image and collect metadata. (2) Constructing the HawkVision protocol format with the metadata before sending the packets. This part is built on top of DPDK.

Frontend. HawkVision is built on top of Clockwork and modified to support modelless inference with different accuracy requirements provided by the users, as it offers flexible control over model loading and unloading. We developed a network protocol and JPEG recovery component with DPDK, allowing us to support lossy inference and recover images from corruption in JPEG format.

Backend. We built a proxy for the backend that can link to any serving system. It uses a reliable protocol and provides high-speed send/receive services to the clients. When requests are received, the images are directed to the inference serving system. We use Clockwork as the serving system for all experiments. It also works with other inference engines, such as NVIDIA’s Triton Inference Server [11], as an alternative. Additionally, the proxy has a channel to handle frontend notifications. When the proxy receives messages from the frontend, it coordinates GPU interruption or removes requests from the GPU queue according to different modes of HawkVision.

6.2 FPGA frontend Prototype

Power consumption is important at the edge. Although our system is developed with GPUs, we also implemented an FPGA prototype to prove our designs of *confidence scaling* and *lossy JPEG recovery* on an FPGA, as shown in Figure 11. Our FPGA prototype is designed to demonstrate the power consumption and performance benefits by implementing the entire inference pipeline to support modelless serving. This can be applied to a dedicated edge-DC case that accepts one application enabled at a time.

We use the Xilinx Alveo U250 FPGA [13] as our development board. The board is equipped with 2x QSFP28 network interfaces. The inference model complies with the modified FPGA AI model compiler FINN [20, 71] so that the model can output both answers and probability vectors. The FPGA

JPEG decoder is sourced from an open-source solution [4]. For other components, we write P4 [21], C++ (Vitis HLS [14]), and Verilog for different purposes to generate the final RTL code. The Vivado [15] and Vitis HLS versions used are 2021.2.

The only functional difference between the FPGA prototype and the GPU-based frontend is the support for swapping. We did not implement swapping in the FPGA, as it is used for demonstrating the pipeline and the two core ideas. Consequently, the prototype supports only one application at a time (one small model in the FPGA frontend and one large model in the GPU backend). We discuss the implementation of the FPGA prototype in the next section.

Our FPGA frontend runs a series of modules to process packets sequentially in a pipeline:

- **Traffic manager.** The manager duplicates incoming packets before forwarding them to the GPU. It ignores any non-HawkVision-related packets and HawkVision-related but retransmitted packets to the frontend.
- **JPEG recovery stack.** The recovery module detects packet loss and recovers the JPEG image when loss happens. It fills the lost information with pixels already received so that the FPGA can continue inference rather than dropping the image due to lost packets.
- **Image preprocessor.** The decoder decodes a JPEG byte stream into a raw RGB data stream. The preprocessor bridges the format mismatch between the raw RGB data stream and the input requirements of the inference model. Image resizing and cropping are performed in this module.
- **Inference model.** The FPGA uses a simpler but faster model to accelerate the inference task. To ensure good overall accuracy, the model pushes the inference result and the corresponding confidence score out for final judgment at the result arbiter. In the GPU solution, this part is replaced by a model pool that can be swapped in and out to support multi-tenancy.
- **Result arbiter.** The arbiter maintains a model-specific confidence score threshold. If a result’s confidence is above the threshold, it sends the result to the client and generates a terminate packet to the GPU to cancel the corresponding inference request. Both packets are sent using UDP and require no confirmation. Otherwise, the arbiter discards the result and lets the GPU finish.

7 Evaluation

HawkVision demonstrates improvement with up to $1.6\times$ P90 improvement compared to the baseline for serving applications with three different GPU and multi-tenancy settings. Our FPGA prototype improves latency and power consumption by up to $1.5\times$ and $3.34\times$, respectively, compared to the

A100. We also demonstrate the feasibility of our FPGA prototype performing lossy inference under severe packet loss. Additionally, we report the implementation resource details of HawkVision with FPGA.

7.1 Experimental Setup

We evaluate HawkVision in an edge-DC setting. To replicate edge-internet settings, we use the Linux *tc* tool to add the edge delay from the client to the frontend and the internet delay to the backend, simulating real cases similar to previous work [76]. Our default setting uses 3ms and 10ms as edge and internet delays, respectively. For both the frontend and backend, we use NVIDIA A100 GPUs but limit the memory usage to a range from 4GB to 16GB to reflect typical settings for edge hardware accelerators [10, 57].

We target the image classification task using the ImageNet [29] dataset, which includes around 50K images. We use a uniform random distribution as the workload distribution for users to send different accuracy requirements.

For the FPGA prototype (HawkVision-FPGA), we built our system on an AMD Xilinx U250 FPGA to demonstrate the performance and power benefits and show the feasibility of hardware-friendly packet loss recovery and confidence scaling implemented in FPGA.

Baselines. We pick Clockwork [34] as our main baseline. Clockwork is a state-of-the-art inference serving system that schedules incoming user requests to different GPU instances with the goal of maintaining predictable performance. We apply Clockwork in the edge-DC setting by scheduling requests on two GPUs, one as the edge and one as the DC GPU. Since Clockwork targets a homogeneous GPU setting, we set the edge GPU and the DC GPU to have the same GPU memory size to make a fair comparison.

For the FPGA implementation, we use both T4 and A100 GPUs for comparison, to show the performance and power consumption with different accelerator options.

Metrics. We report (1) the average latency, as well as latencies at P90, P99, and P100 for all inferences in the system. Tail latency, crucial for meeting Service Level Objective (SLO) requirements in inference serving [34], is one of our main motivations for optimizing latency. (2) Power consumption, which is important for edge settings with limited power constraints. We compare the power efficiency among hardware accelerators, and we also report the FPGA resources used in our implemented prototype.

7.2 HawkVision Reduces Swapping Cost

We compare the edge-DC systems with HawkVision and the traditional model separation scheme in Clockwork. We configure three different settings in terms of the number of applications and GPU memory for the edge-DC systems (2 GPUs) to serve: (4GB, 25 applications), (8GB, 50 applications),

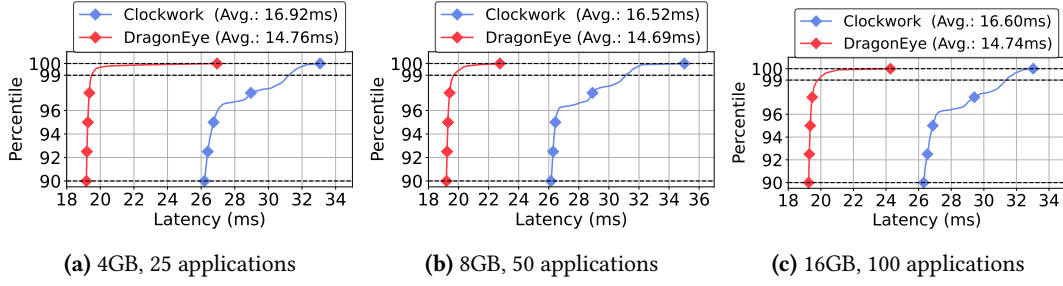


Figure 12. Latency percentiles of three settings

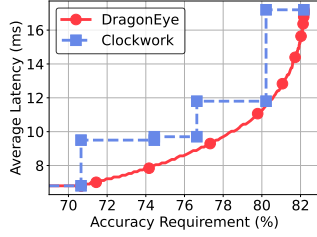


Figure 13. Latency curve with different accuracy requirement

and (16GB, 100 applications). For each application, we use 5 models with different accuracy profiles to meet various accuracy requirements from different users, ranging from 70% to 85%, as aligned with [35].

Figure 12 shows the latency performance for these 3 settings. Taking Figure 12a as an example, 25 applications each with 5 models (totaling $25 * 5 = 125$ models) will participate in the inference. When the system receive the request, the corresponding models will first be loaded into the memory if they do not already exist, thereby incurring swapping latency. HawkVision reduces the number of models from 125 to 50 because each application needs only two models to cover the accuracy requirement spectrum.

In the 25 application settings (Figure 12a), HawkVision achieves both better tail latency and average latency compared to Clockwork, outperforming it by 1.36X, 1.6X, and 1.22X in P90, P99, and P100, respectively. HawkVision also surpasses Clockwork by 1.14X in average latency. The trends observed in the 50 (Figure 12b) and 100 (Figure 12c) application settings are similar.

7.3 HawkVision Uses Request-level Granularity

We take a deeper look into the the latency for different accuracy requirements using request-level granularity (HawkVision) and model-level granularity (Clockwork). For Clockwork, system selects the model with lowest accuracy that could serve the accuracy requirement from the user request.

For Clockwork, we select 5 models with the accuracy identical to previous work [35]. For HawkVision, we select the

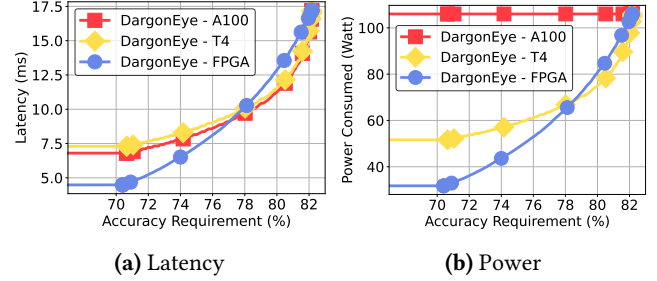


Figure 14. Different hardware with different latency and power consumption.

highest accuracy and lowest accuracy models among the five: *winograd_resnet18_v2* and *resnet101*.

Figure 13 demonstrates the latency benefits. In HawkVision, latency varies according to different accuracy requirements because different proportions of requests are sent to the backend with confidence scaling. When frontend inference confidence is insufficient, requests fall back to the backend GPU. For instance, at an accuracy requirement of 75%, approximately 96% of requests are replied to by the edge vision box in HawkVision. However, in a separate model deployment scenario (Clockwork), all requests below a certain accuracy requirement are sent to the closest model which can serve the target accuracy requirement, resulting in high overhead due to serving with overkill models, causing a 0.84X worse performance compared to HawkVision.

Confidence scaling requires only two models with their confidence scores presented. Since the edge is a relatively power-constrained environment, deploying power-hungry hardware like the A100 is challenging. Therefore, both performance and power are important considerations. To address this issue, we implemented an FPGA prototype. Because *winograd_resnet18_v2* cannot be directly deployed to the FPGA, we selected MobileNet, compiled using Xilinx FINN [71], which achieves the same accuracy for a fair comparison.

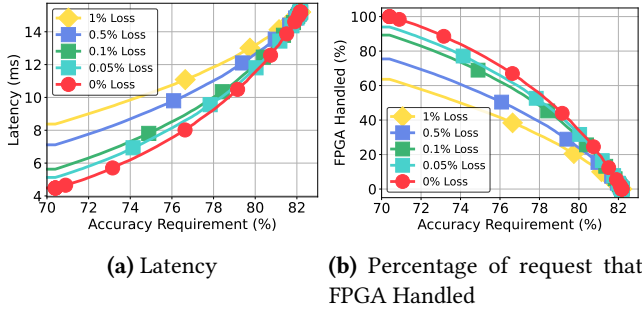


Figure 15. Encountering different packet loss rate.

In Figure 14a, we show that the FPGA achieves similar performance to the A100 and T4 at the edge device and outperforms the A100 by 1.5X with the FPGA solution. The performance benefits come from the image processing pipeline and streaming advantages in FPGA architecture. In Figure 14b, we can see that the power consumption when using the A100 for the edge is high, with an average of 106W at a 70% accuracy requirement, while this number decreases to 31.74W with the FPGA prototype, showing a 3.34X reduction in power consumption with the FPGA.

7.4 HawkVision Handles Packet Loss

Packet loss causes long network delays and significantly impacts performance. HawkVision designs a hardware-friendly, streaming-based JPEG recovery scheme that enables lossy inference when packet loss occurs. Figures 15a and 15b demonstrate that when HawkVision-FPGA encounters various levels of packet loss, it can still function effectively, perform recovery, and make lossy inferences. Our confidence scaling design allows unconfident results due to lossy inference to fall back to the DC backend for handling requests. When 1% packet loss is encountered, the overall latency increases from 4.48ms to 8.2ms, representing approximately a 1.83X degradation. This increase is because, while we can handle lossy inference, achieving the same accuracy for client service without quality loss requires more requests (37% of the requests for 75% accuracy) to fall back to the backend for inference.

7.5 Resource Utilization of HawkVision-FPGA

We now report HawkVision power usage compared to GPU solutions and HawkVision resource usage on FPGA.

Power Consumption. Our system has lower power consumption compared to GPU solutions. HawkVision consumes only 31.74W when it is active. In comparison, an A100 GPU consumes an average of 56W when idle, and this number increases to an average of 106W when making inference requests with the same configuration and a batch size of 1. At maximum load, the power consumption can go up to 250W-400W [8].

FPGA Resource utilization Table 1 shows the FPGA resource utilization of HawkVision and OpenNIC in our implementation on Xilinx Alveo U250 FPGA Card. The percentages and numbers on the table represent the usage of different types of resources on the FPGA.

The OpenNIC provides the basic network functions to drive the FPGA to send and receive packets with the QSFP28 network interface. The whole HawkVision workflow is developed inside the OpenNIC skeleton. Our system uses 26% more LUT, 8% more FF, and 53% more BRAM compared to OpenNIC.

The table also indicates that we still have available space to potentially add additional functions to the FPGA, introduce other models, or migrate our entire design to a low-end FPGA for better cost savings. This is feasible given that CV models are typically small, and advancements in quantization and sparsification techniques continue to reduce the size of the models. As mentioned in Xilinx FINN [16], a VGG-16-like model can be accommodated on a Pynq-Z1 board to further reduce power consumption.

8 Related Work

Minimizing Inference System Cost. To minimize serving costs, static provisioning alone is not sufficient [11, 56]. Recent works propose model scheduling and resource scaling on GPUs based on their application requirements in real-time [34, 63], serving inferences in cost-effective spot instances with fault tolerance considerations [35], or sacrificing model accuracy when serving demand is high, rather than scaling up hardware resources to serve models [17], all aimed at helping minimize serving costs.

Hardware Acceleration for ML. Many hardware solutions have been proposed because of the increasing demand for accelerating machine learning training and inference applications. Notably many solutions focus on using FPGAs as AI accelerators [12, 20, 26, 33, 37, 39, 51, 51, 54, 58, 71, 73, 80]. N3IC [67] uses a SmartNIC to help machine learning inference. Taurus [68], SwitchML [65], ATP [46] and other works [64, 75] discuss the possibility offload machine learning applications to the network programmable switches. None of these approaches consider a middlebox-style approach where FPGA adds functionality to an end-to-end inference pipeline.

Reducing both network and data processing taxes. While previous work has primarily focused on improving model inference times through better resource scheduling within data centers [28, 34, 35, 63, 78], or optimizing the models themselves [20, 26, 37, 39, 51, 51, 58, 71, 73, 80], a significant portion of the end-to-end inference delay originates from network and data processing taxes, which have not been well-addressed. To reduce these taxes, we adopt a middlebox-based lossy inference service that resides closer

Resources	OpenNIC		HawkVision	
	Percentage	Numbers	Percentage	Numbers
LUT	6%	99638	32%	328282
LUTRAM	2%	13781	8%	65563
FF	4%	144632	12%	423430
BRAM	7%	178	60%	1620.5
URAM	1%	10	3%	32
DSP	0%	0	3%	156

Table 1. the FPGA resource usage of HawkVision and the NIC skeleton

to the user’s device, minimizing the impact of network delays and packet losses within the network. Furthermore, in an environment where edge devices often have limited energy resources [42, 57], designing such a low-energy inference middlebox with the capability to perform all the necessary functionalities shown in Figure 3 and directly answer inference queries has never been cost-effective. In the following section, we introduce our full-fledged middlebox solution featuring a lower-power FPGA.

9 Discussion

9.1 Applies HawkVision to Language-based Tasks

While HawkVision is demonstrated with vision models in this paper, the contributions apply equally well to language processing models. Recent research [48, 74] has explored the confidence of answers output from large language models (LLMs) by instructing the models to output the confidence or the quality of the results. The findings are similar to those in §4.2, where higher confidence corresponds to better evaluation results. Moreover, although there are no publicly available LLM inference deployments for FPGA at this time, recent developments in deploying LLMs to FPGA for inference are making progress [24]. With these advancements, the FPGA frondend and the backend server can adapt to different tasks, following the hierarchical design of HawkVision. By adjusting the confidence threshold, HawkVision can control the quality or accuracy of tasks, ensuring flexibility and efficiency across various applications.

9.2 Inference Model on FPGA

In recent years, there have been many works [26, 37, 39, 51, 51, 58, 73, 80] proposed to accelerate inference using FPGAs. There has been a range of advances that have progressively packed complex models on to FPGAs with low memory footprint and low latency, while minimally compromising accuracy. For example, prior research [23, 25, 27, 31, 41, 43, 59, 60] shows that applying quantization to models can greatly accelerate FPGA inference speed via simplified models, while still maintaining a good level of accuracy, even when using a binary representation of the parameters. Furthermore,

previous work has shown that we can remove the redundant parameters that do not contribute much to the accuracy [32, 40, 45, 47]. This can not only improve inference throughput, but also reduce the model’s memory footprint and allow the FPGA to host a more sophisticated model(s). Solutions such as [45, 51] further accelerate the FPGA inference pipeline by converting the model into a streamlined architecture. Furthermore, operator fusion [20, 71] can be used to merge complex operators (e.g. floating-point operations) at compile time for even greater speed. Our work can leverage all these advances when hosting models on the FPGA with the goal of keeping the FPGA model’s accuracy close to the GPU-resident model, yet simple so as to yield tangible memory and performance improvements. No matter the advances, there will likely be an FPGA-GPU model accuracy gap, so we need an approach to bridge the outcome of that gap. We discuss this next.

10 Conclusion

We built HawkVision, an edge-DC system where the frontend supports JPEG recovery and lossy inference in client requests. It also applies confidence scaling with the backend to support a wide range of accuracy requirements, achieving better performance gains and reducing deployment costs. Our FPGA prototype also demonstrates the feasibility of implementing this system in a more power-efficient way.

References

- [1] Amazon EC2 Inf1 Instances. https://aws.amazon.com/ec2/instance-types/inf1/?nc1=h_ls.
- [2] AWS Machine Learning Blog. <https://aws.amazon.com/blogs/machine-learning/reduce-ml-inference-costs-on-amazon-sagemaker-for-pytorch-models-using-amazon-bif>
- [3] BIF Source Code. <https://github.com/bif-nsdi23/bif-nsdi23>.
- [4] High throughput JPEG decoder Github Repository. https://github.com/ultraembedded/core_jpeg.
- [5] libjpeg-turbo Github Repository. <https://github.com/libjpeg-turbo/libjpeg-turbo>.
- [6] Live Video Analytics with Microsoft Rocket for reducing edge compute costs. <https://techcommunity.microsoft.com/t5/internet-of-things-blog/live-video-analytics-with-microsoft-rocket-for-reducing-edge/ba-p/1522305>.

- [7] Microsoft and AT&T demonstrate 5G-powered video analytics. <https://azure.microsoft.com/en-us/blog/microsoft-and-att-demonstrate-5g-powered-video-analytics/>.
- [8] NVIDIA A100 TENSOR CORE GPU. <https://www.nvidia.com/content/dam/en-zz/Solutions/Data-Center/a100/pdf/nvidia-a100-datasheet-us-nvidia-1758950-r4-web.pdf>.
- [9] NVIDIA DALI. <https://docs.nvidia.com/deeplearning/dali/user-guide/docs/#>.
- [10] NVIDIA Jetson: The AI platform for edge computing. <https://www.nvidia.com/en-us/autonomous-machines/embedded-systems/>.
- [11] NVIDIA TRITON INFERENCE SERVER. <https://developer.nvidia.com/nvidia-triton-inference-server>.
- [12] Vitis AI. <https://www.xilinx.com/products/design-tools/vitis/vitis-ai.html>.
- [13] Xilinx Alveo U250 Data Center Accelerator Card. <https://www.xilinx.com/products/boards-and-kits/alveo/u250.html>.
- [14] Xilinx Vitis High Level Synthesis (HLS) tool. <https://www.xilinx.com/support/documentation/navigation/design-hubs/2020-2/dh0090-vitis-hls-hub.html>.
- [15] Xilinx Vivado® Design Suite. <https://www.xilinx.com/products/design-tools/vivado.html>.
- [16] Xilinx FINN Github. <https://github.com/Xilinx/finn-examples>.
- [17] Sohaib Ahmad, Hui Guan, Brian D Friedman, Thomas Williams, Ramesh K Sitaraman, and Thomas Woo. Proteus: A high-throughput inference-serving system with accuracy scaling. ASPLOS '24. Association for Computing Machinery, 2024.
- [18] Romil Bhardwaj, Zhengxu Xia, Ganesh Ananthanarayanan, Junchen Jiang, Yuanhao Shu, Nikolaos Karianakis, Kevin Hsieh, Paramvir Bahl, and Ion Stoica. Ekya: Continuous learning of video analytics models on edge compute servers. In *19th USENIX Symposium on Networked Systems Design and Implementation (NSDI 22)*, pages 119–135, Renton, WA, April 2022. USENIX Association.
- [19] Apurv Bhartiya, Bo Chen, Feng Wang, Derrick Pallas, Raluca Musaloiu-E, Ted Tsung-Te Lai, and Hao Ma. Measurement-based, practical techniques to improve 802.11ac performance. In *Proceedings of the 2017 Internet Measurement Conference, IMC '17*, page 205–219, New York, NY, USA, 2017. Association for Computing Machinery.
- [20] Michaela Blott, Thomas B Preußer, Nicholas J Fraser, Giulio Gambardella, Kenneth O'brien, Yaman Umuroglu, Miriam Leiser, and Kees Viessers. Finn-r: An end-to-end deep-learning framework for fast exploration of quantized neural networks. *ACM Transactions on Reconfigurable Technology and Systems (TRETS)*, 11(3):1–23, 2018.
- [21] Pat Bosshart, Dan Daly, Glen Gibb, Martin Izzard, Nick McKeown, Jennifer Rexford, Cole Schlesinger, Dan Talayco, Amin Vahdat, George Varghese, and David Walker. P4: Programming protocol-independent packet processors. *SIGCOMM Comput. Commun. Rev.*, 44(3):87–95, jul 2014.
- [22] Tom B. Brown, Benjamin Mann, Nick Ryder, Melanie Subbiah, Jared Kaplan, Prafulla Dhariwal, Arvind Neelakantan, Pranav Shyam, Girish Sastry, Amanda Askell, Sandhini Agarwal, Ariel Herbert-Voss, Gretchen Krueger, Tom Henighan, Rewon Child, Aditya Ramesh, Daniel M. Ziegler, Jeffrey Wu, Clemens Winter, Christopher Hesse, Mark Chen, Eric Sigler, Mateusz Litwin, Scott Gray, Benjamin Chess, Jack Clark, Christopher Berner, Sam McCandlish, Alec Radford, Ilya Sutskever, and Dario Amodei. Language models are few-shot learners. In *Proceedings of the 34th International Conference on Neural Information Processing Systems, NIPS'20*, Red Hook, NY, USA, 2020. Curran Associates Inc.
- [23] Zhaowei Cai, Xiaodong He, Jian Sun, and Nuno Vasconcelos. Deep learning with low precision by half-wave gaussian quantization. In *Proceedings of the IEEE Conference on Computer Vision and Pattern Recognition (CVPR)*, July 2017.
- [24] Hongzheng Chen, Jiahao Zhang, Yixiao Du, Shaojie Xiang, Zichao Yue, Niansong Zhang, Yaohui Cai, and Zhiru Zhang. Understanding the potential of fpga-based spatial acceleration for large language model inference. *ACM Trans. Reconfigurable Technol. Syst.*, apr 2024. Just Accepted.
- [25] Tianlong Chen, Zhenyu Zhang, Xu Ouyang, Zechun Liu, Zhiqiang Shen, and Zhangyang Wang. "bnn - bn = ?": Training binary neural networks without batch normalization. In *Proceedings of the IEEE/CVF Conference on Computer Vision and Pattern Recognition (CVPR) Workshops*, pages 4619–4629, June 2021.
- [26] Yao Chen, Jiong He, Xiaofan Zhang, Cong Hao, and Deming Chen. Cloud-dnn: An open framework for mapping dnn models to cloud fpgas. In *Proceedings of the 2019 ACM/SIGDA International Symposium on Field-Programmable Gate Arrays, FPGA '19*, page 73–82, New York, NY, USA, 2019. Association for Computing Machinery.
- [27] Matthieu Courbariaux and Yoshua Bengio. Binarynet: Training deep neural networks with weights and activations constrained to +1 or -1. *CoRR*, abs/1602.02830, 2016.
- [28] Daniel Crankshaw, Xin Wang, Guilio Zhou, Michael J. Franklin, Joseph E. Gonzalez, and Ion Stoica. Clipper: A low-latency online prediction serving system. In *14th USENIX Symposium on Networked Systems Design and Implementation (NSDI 17)*, pages 613–627, Boston, MA, March 2017. USENIX Association.
- [29] Jia Deng, Wei Dong, Richard Socher, Li-Jia Li, Kai Li, and Li Fei-Fei. Imagenet: A large-scale hierarchical image database. In *2009 IEEE Conference on Computer Vision and Pattern Recognition*, pages 248–255, 2009.
- [30] Kuntai Du, Ahsan Pervaiz, Xin Yuan, Aakanksha Chowdhery, Qizheng Zhang, Henry Hoffmann, and Junchen Jiang. Server-driven video streaming for deep learning inference. In *Proceedings of the Annual Conference of the ACM Special Interest Group on Data Communication on the Applications, Technologies, Architectures, and Protocols for Computer Communication, SIGCOMM '20*, page 557–570, New York, NY, USA, 2020. Association for Computing Machinery.
- [31] Jun Fang, Ali Shafiee, Hamzah Abdel-Aziz, David Thorsley, Georgios Georgiadis, and Joseph H. Hassoun. Post-training piecewise linear quantization for deep neural networks. In Andrea Vedaldi, Horst Bischof, Thomas Brox, and Jan-Michael Frahm, editors, *Computer Vision – ECCV 2020*, pages 69–86, Cham, 2020. Springer International Publishing.
- [32] Jonathan Frankle and Michael Carbin. The lottery ticket hypothesis: Finding sparse, trainable neural networks. *arXiv preprint arXiv:1803.03635*, 2018.
- [33] Nadeen Gebara, Manya Ghobadi, and Paolo Costa. In-network aggregation for shared machine learning clusters. In A. Smola, A. Dimakis, and I. Stoica, editors, *Proceedings of Machine Learning and Systems*, volume 3, pages 829–844, 2021.
- [34] Arpan Gujarati, Reza Karimi, Safya Alzayat, Wei Hao, Antoine Kaufmann, Ymir Vigfusson, and Jonathan Mace. Serving dnns like clockwork: Performance predictability from the bottom up. In *14th USENIX Symposium on Operating Systems Design and Implementation (OSDI 20)*, pages 443–462. USENIX Association, November 2020.
- [35] Jashwant Raj Gunasekaran, Cyan Subhra Mishra, Prashanth Thinnakaran, Bikash Sharma, Mahmut Taylan Kandemir, and Chita R. Das. Cocktail: A multidimensional optimization for model serving in cloud. In *19th USENIX Symposium on Networked Systems Design and Implementation (NSDI 22)*, pages 1041–1057, Renton, WA, April 2022. USENIX Association.
- [36] Chuan Guo, Geoff Pleiss, Yu Sun, and Kilian Q. Weinberger. On calibration of modern neural networks. In Doina Precup and Yee Whye Teh, editors, *Proceedings of the 34th International Conference on Machine Learning*, volume 70 of *Proceedings of Machine Learning Research*,

- pages 1321–1330. PMLR, 06–11 Aug 2017.
- [37] Kaiyuan Guo, Shulin Zeng, Jincheng Yu, Yu Wang, and Huazhong Yang. [dl] a survey of fpga-based neural network inference accelerators. *ACM Trans. Reconfigurable Technol. Syst.*, 12(1), mar 2019.
 - [38] Peizhen Guo, Bo Hu, and Wenjun Hu. Sommelier: Curating dnn models for the masses. In *Proceedings of the 2022 International Conference on Management of Data*, SIGMOD '22, page 1876–1890, New York, NY, USA, 2022. Association for Computing Machinery.
 - [39] Mathew Hall and Vaughn Betz. HPIPE: Heterogeneous layer-pipelined and sparse-aware CNN inference for FPGAs. *arXiv preprint arXiv:2007.10451*, 2020.
 - [40] Song Han, Jeff Pool, John Tran, and William Dally. Learning both weights and connections for efficient neural network. In C. Cortes, N. Lawrence, D. Lee, M. Sugiyama, and R. Garnett, editors, *Advances in Neural Information Processing Systems*, volume 28. Curran Associates, Inc., 2015.
 - [41] Itay Hubara, Matthieu Courbariaux, Daniel Soudry, Ran El-Yaniv, and Yoshua Bengio. Binarized neural networks. In D. Lee, M. Sugiyama, U. Luxburg, I. Guyon, and R. Garnett, editors, *Advances in Neural Information Processing Systems*, volume 29. Curran Associates, Inc., 2016.
 - [42] Mehrdad Khani, Ganesh Ananthanarayanan, Kevin Hsieh, Junchen Jiang, Ravi Netravali, Yuanchao Shu, Mohammad Alizadeh, and Victor Bahl. RECL: Responsive Resource-Efficient continuous learning for video analytics. In *20th USENIX Symposium on Networked Systems Design and Implementation (NSDI 23)*, pages 917–932, Boston, MA, April 2023. USENIX Association.
 - [43] Minje Kim and Paris Smaragdis. Bitwise neural networks. *arXiv preprint arXiv:1601.06071*, 2016.
 - [44] Young Geun Kim, Udit Gupta, Andrew McCrabb, Yonglak Son, Valeria Bertacco, David Brooks, and Carole-Jean Wu. Greenscale: Carbon-aware systems for edge computing. *arXiv preprint arXiv:2304.00404*, 2023.
 - [45] H.T. Kung, Bradley McDanel, and Sai Qian Zhang. Packing sparse convolutional neural networks for efficient systolic array implementations: Column combining under joint optimization. In *Proceedings of the Twenty-Fourth International Conference on Architectural Support for Programming Languages and Operating Systems*, ASPLOS '19, page 821–834, New York, NY, USA, 2019. Association for Computing Machinery.
 - [46] ChonLam Lao, Yanfang Le, Kshiteej Mahajan, Yixi Chen, Wenfei Wu, Aditya Akella, and Michael Swift. ATP: In-network aggregation for multi-tenant learning. In *18th USENIX Symposium on Networked Systems Design and Implementation (NSDI 21)*, pages 741–761. USENIX Association, April 2021.
 - [47] Hao Li, Asim Kadav, Igor Durdanovic, Hanan Samet, and Hans Peter Graf. Pruning filters for efficient convnets. *arXiv preprint arXiv:1608.08710*, 2016.
 - [48] Moxin Li, Wenjie Wang, Fuli Feng, Fengbin Zhu, Qifan Wang, and Tat-Seng Chua. Think twice before assure: Confidence estimation for large language models through reflection on multiple answers, 2024.
 - [49] Zhuohan Li, Lianmin Zheng, Yinmin Zhong, Vincent Liu, Ying Sheng, Xin Jin, Yanping Huang, Zhifeng Chen, Hao Zhang, Joseph E. Gonzalez, and Ion Stoica. AlpaServe: Statistical multiplexing with model parallelism for deep learning serving. In *17th USENIX Symposium on Operating Systems Design and Implementation (OSDI 23)*, pages 663–679, Boston, MA, July 2023. USENIX Association.
 - [50] Zhuang Liu, Hanzi Mao, Chao-Yuan Wu, Christoph Feichtenhofer, Trevor Darrell, and Saining Xie. A convnet for the 2020s. In *Proceedings of the IEEE/CVF Conference on Computer Vision and Pattern Recognition (CVPR)*, pages 11976–11986, June 2022.
 - [51] Bradley McDanel, Sai Qian Zhang, H. T. Kung, and Xin Dong. Full-stack optimization for accelerating cnns using powers-of-two weights with fpga validation. In *Proceedings of the ACM International Conference on Supercomputing*, ICS '19, page 449–460, New York, NY, USA, 2019. Association for Computing Machinery.
 - [52] Zili Meng, Xiao Kong, Jing Chen, Bo Wang, Mingwei Xu, Rui Han, Honghao Liu, Venkat Arun, Hongxin Hu, and Xue Wei. Hairpin: Rethinking packet loss recovery in edge-based interactive video streaming. In *21st USENIX Symposium on Networked Systems Design and Implementation (NSDI 24)*, Santa Clara, CA, April 2024. USENIX Association.
 - [53] Matthias Minderer, Josip Djolonga, Rob Romijnders, Frances Hubis, Xi-aohua Zhai, Neil Houlsby, Dustin Tran, and Mario Lucic. Revisiting the calibration of modern neural networks. In M. Ranzato, A. Beygelzimer, Y. Dauphin, P.S. Liang, and J. Wortman Vaughan, editors, *Advances in Neural Information Processing Systems*, volume 34, pages 15682–15694. Curran Associates, Inc., 2021.
 - [54] Hiroki Nakahara, Haruyoshi Yonekawa, Tomoya Fujii, and Shimpei Sato. A lightweight yolov2: A binarized cnn with a parallel support vector regression for an fpga. In *Proceedings of the 2018 ACM/SIGDA International Symposium on Field-Programmable Gate Arrays*, FPGA '18, page 31–40, New York, NY, USA, 2018. Association for Computing Machinery.
 - [55] Maxim Naumov, Dheevatsa Mudigere, Hao-Jun Michael Shi, Jianyu Huang, Narayanan Sundaraman, Jongsoo Park, Xiaodong Wang, Udit Gupta, Carole-Jean Wu, Alisson G Azzolini, et al. Deep learning recommendation model for personalization and recommendation systems. *arXiv preprint arXiv:1906.00091*, 2019.
 - [56] Christopher Olston, Noah Fiedel, Kiril Gorovoy, Jeremiah Harmsen, Li Lao, Fangwei Li, Vinu Rajashekhar, Sukriti Ramesh, and Jordan Soyke. Tensorflow-serving: Flexible, high-performance ml serving. *arXiv preprint arXiv:1712.06139*, 2017.
 - [57] Arthi Padmanabhan, Neil Agarwal, Anand Iyer, Ganesh Ananthanarayanan, Yuanchao Shu, Nikolaos Karianakis, Guoqing Harry Xu, and Ravi Netravali. Gemel: Model merging for Memory-Efficient, Real-Time video analytics at the edge. In *20th USENIX Symposium on Networked Systems Design and Implementation (NSDI 23)*, pages 973–994, Boston, MA, April 2023. USENIX Association.
 - [58] Lucian Petrica, Tobias Alonso, Mairin Kroes, Nicholas J. Fraser, Sorin Cotozana, and Michaela Blott. Memory-efficient dataflow inference for deep cnns on FPGA. In *International Conference on Field-Programmable Technology, (IC)FPT 2020, Maui, HI, USA, December 9-11, 2020*, pages 48–55. IEEE, 2020.
 - [59] Haotong Qin, Ruihao Gong, Xianglong Liu, Xiao Bai, Jingkuan Song, and Nicu Sebe. Binary neural networks: A survey. *Pattern Recognition*, 105:107281, 2020.
 - [60] Mohammad Rastegari, Vicente Ordonez, Joseph Redmon, and Ali Farhadi. Xnor-net: Imagenet classification using binary convolutional neural networks. In Bastian Leibe, Jiri Matas, Nicu Sebe, and Max Welling, editors, *Computer Vision – ECCV 2016*, pages 525–542, Cham, 2016. Springer International Publishing.
 - [61] Vijay Janapa Reddi, Christine Cheng, David Kanter, Peter Mattson, Guenther Schmuelling, Carole-Jean Wu, Brian Anderson, Maximilien Breughe, Mark Charlebois, William Chou, Ramesh Chukka, Cody Coleman, Sam Davis, Pan Deng, Greg Diamos, Jared Duke, Dave Fick, J. Scott Gardner, Itay Hubara, Sachin Idgunji, Thomas B. Jablin, Jeff Jiao, Tom St. John, Pankaj Kanwar, David Lee, Jeffery Liao, Anton Lokhov, Francisco Massa, Peng Meng, Paulius Micikevicius, Colin Osborne, Gennady Pekhimenko, Arun Tejusve Raghunath Rajan, Dilip Sequeira, Ashish Sirasao, Fei Sun, Hanlin Tang, Michael Thomson, Frank Wei, Ephrem Wu, Lingjie Xu, Koichi Yamada, Bing Yu, George Yuan, Aaron

- Zhong, Peizhao Zhang, and Yuchen Zhou. Mlperf inference benchmark. In *2020 ACM/IEEE 47th Annual International Symposium on Computer Architecture (ISCA)*, pages 446–459, 2020.
- [62] Joseph Redmon, Santosh Divvala, Ross Girshick, and Ali Farhadi. You only look once: Unified, real-time object detection. In *Proceedings of the IEEE Conference on Computer Vision and Pattern Recognition (CVPR)*, June 2016.
- [63] Francisco Romero, Qian Li, Neeraja J. Yadwadkar, and Christos Kozyrakis. INFaaS: Automated model-less inference serving. In *2021 USENIX Annual Technical Conference (USENIX ATC 21)*, pages 397–411. USENIX Association, July 2021.
- [64] Davide Sanvito, Giuseppe Siracusano, and Roberto Bifulco. Can the network be the ai accelerator? In *Proceedings of the 2018 Morning Workshop on In-Network Computing*, NetCompute '18, page 20–25, New York, NY, USA, 2018. Association for Computing Machinery.
- [65] Amedeo Sapio, Marco Canini, Chen-Yu Ho, Jacob Nelson, Panos Kalnis, Changhoon Kim, Arvind Krishnamurthy, Masoud Moshref, Dan Ports, and Peter Richtarik. Scaling distributed machine learning with in-network aggregation. In *18th USENIX Symposium on Networked Systems Design and Implementation (NSDI 21)*, pages 785–808. USENIX Association, April 2021.
- [66] Sudipta Saha Shubha and Haiying Shen. Adainf: Data drift adaptive scheduling for accurate and slo-guaranteed multiple-model inference serving at edge servers. In *Proceedings of the ACM SIGCOMM 2023 Conference*, ACM SIGCOMM '23, page 473–485, New York, NY, USA, 2023. Association for Computing Machinery.
- [67] Giuseppe Siracusano, Salvator Galea, Davide Sanvito, Mohammad Malekzadeh, Gianni Antichi, Paolo Costa, Hamed Haddadi, and Roberto Bifulco. Re-architecting traffic analysis with neural network interface cards. In *19th USENIX Symposium on Networked Systems Design and Implementation (NSDI 22)*, pages 513–533, Renton, WA, April 2022. USENIX Association.
- [68] Tushar Swamy, Alexander Rucker, Muhammad Shahbaz, and Kunle Olukotun. Taurus: An intelligent data plane. *arXiv preprint arXiv:2002.08987*, 2020.
- [69] Hugo Touvron, Thibaut Lavril, Gautier Izacard, Xavier Martinet, Marie-Anne Lachaux, Timothée Lacroix, Baptiste Rozière, Naman Goyal, Eric Hambro, Faisal Azhar, et al. Llama: Open and efficient foundation language models. *arXiv preprint arXiv:2302.13971*, 2023.
- [70] Hugo Touvron, Louis Martin, Kevin Stone, Peter Albert, Amjad Almahairi, Yasmine Babaei, Nikolay Bashlykov, Soumya Batra, Prajjwal Bhargava, Shruti Bhosale, et al. Llama 2: Open foundation and fine-tuned chat models. *arXiv preprint arXiv:2307.09288*, 2023.
- [71] Yaman Umuroglu, Nicholas J. Fraser, Giulio Gambardella, Michaela Blott, Philip Leong, Magnus Jahre, and Kees Vissers. Finn: A framework for fast, scalable binarized neural network inference. In *Proceedings of the 2017 ACM/SIGDA International Symposium on Field-Programmable Gate Arrays*, FPGA '17, pages 65–74. ACM, 2017.
- [72] Nikita Vemuri. Scoring confidence in neural networks. Master's thesis, EECS Department, University of California, Berkeley, Jun 2020.
- [73] Lixue Xia, Lansong Diao, Zhao Jiang, Hao Liang, Kai Chen, Li Ding, Shunli Dou, Zibin Su, Meng Sun, Jiansong Zhang, and Wei Lin. Pai-fcnn: Fpga based inference system for complex cnn models. In *2019 IEEE 30th International Conference on Application-specific Systems, Architectures and Processors (ASAP)*, volume 2160-052X, pages 107–114, 2019.
- [74] Miao Xiong, Zhiyuan Hu, Xinyang Lu, YIFEI LI, Jie Fu, Junxian He, and Bryan Hooi. Can LLMs express their uncertainty? an empirical evaluation of confidence elicitation in LLMs. In *The Twelfth International Conference on Learning Representations*, 2024.
- [75] Zhaoqi Xiong and Noa Zilberman. Do switches dream of machine learning? toward in-network classification. In *Proceedings of the 18th ACM Workshop on Hot Topics in Networks*, HotNets '19, page 25–33, New York, NY, USA, 2019. Association for Computing Machinery.
- [76] Ben Zhang, Xin Jin, Sylvia Ratnasamy, John Wawrzynnek, and Edward A. Lee. Awstream: Adaptive wide-area streaming analytics. In *Proceedings of the 2018 Conference of the ACM Special Interest Group on Data Communication*, SIGCOMM '18, page 236–252, New York, NY, USA, 2018. Association for Computing Machinery.
- [77] Chengliang Zhang, Minchen Yu, Wei Wang, and Feng Yan. MARK: Exploiting cloud services for Cost-Effective, SLO-Aware machine learning inference serving. In *2019 USENIX Annual Technical Conference (USENIX ATC 19)*, pages 1049–1062, Renton, WA, July 2019. USENIX Association.
- [78] Hong Zhang, Yupeng Tang, Anurag Khandelwal, and Ion Stoica. SHEPHERD: Serving DNNs in the wild. In *20th USENIX Symposium on Networked Systems Design and Implementation (NSDI 23)*, pages 787–808, Boston, MA, April 2023. USENIX Association.
- [79] Jeff Zhang, Sameh Elnikety, Shuayb Zarar, Atul Gupta, and Siddharth Garg. Model-Switching: Dealing with fluctuating workloads in Machine-Learning-as-a-Service systems. In *12th USENIX Workshop on Hot Topics in Cloud Computing (HotCloud 20)*. USENIX Association, July 2020.
- [80] Sai Qian Zhang, Jieyu Lin, and Qi Zhang. Adaptive distributed convolutional neural network inference at the network edge with adcn. In *49th International Conference on Parallel Processing - ICPP*, ICPP '20, New York, NY, USA, 2020. Association for Computing Machinery.
- [81] Yuhao Zhou, Tingfeng Wang, Liying Wang, Nian Wen, Rui Han, Jing Wang, Chenglei Wu, Jiafeng Chen, Longwei Jiang, Shibo Wang, Honghao Liu, and Chenren Xu. AUGUR: Practical mobile multipath transport service for low tail latency in Real-Time streaming. In *21st USENIX Symposium on Networked Systems Design and Implementation (NSDI 24)*, Santa Clara, CA, April 2024. USENIX Association.